LWT - Food Science and Technology 154 (2022) 112833

Contents lists available at ScienceDirect

LWT

journal homepage: www.elsevier.com/locate/lwt

Characterization of glucose-crosslinked gelatin films reinforced with chitin nanowhiskers for active packaging development

Alaitz Etxabide [a,b,*], Paul A. Kilmartin [b], Juan I. Maté [c,d], Joaquín Gómez-Estaca [e,**]

[a] BIOMAT Research Group, University of the Basque Country (UPV/EHU), Escuela de Ingeniería de Gipuzkoa, Plaza de Europa 1, 20018, Donostia-San Sebastián, Spain
[b] School of Chemical Sciences 302, University of Auckland, 23 Symonds Street, Private Bag 92019, 1010, Auckland, New Zealand
[c] ALITEC Research Group, Department of Agronomy, Biotechnology and Food, School of Agricultural Engineering, Public University of Navarre (upna/nup), 31006, Pamplona-Iruña, Spain
[d] Research Institute for Innovation & Sustainable Development in Food Chain, Department of Agronomy, Biotechnology and Food, Public University of Navarre (upna/nup), 31006, Pamplona-Iruña, Spain
[e] Institute of Food Science, Technology and Nutrition (CSIC), José Antonio Novais 10, 28040, Madrid, Spain

ARTICLE INFO

Keywords:
Gelatin
Chitin nanowhiskers
Maillard reaction
Reinforced films
Active films

ABSTRACT

To find renewable and sustainable alternatives to reduce the severe environmental impact of single-use synthetic plastic packaging, glucose-crosslinked gelatin films containing different amounts of chitin nanowhiskers (CNWs) were prepared. CNWs were first prepared by acid hydrolysis of chitin from shrimps, and characterized (morphological and thermal properties), before their addition into film-forming formulations. The films were heat-treated to promote the chemical crosslinking Maillard reaction (MR), between glucose and gelatin. The films then became less soluble (from 100% to ~10%), thermally more stable, had a notably improved UV–vis light absorption capacity, and presented significantly enhanced tensile strength (from 42 to 77 MPa) and Young's modulus (from 1476 to 2921 MPa), however, they also became less flexible (from 17% to 7%) and transparent. These property alterations were mainly related to changes in crystallinity, the MR and to a lesser extent, to the formation of noncovalent (electrostatic and hydrogen bonding) interactions between CNWs and gelatin. Furthermore, due to the formation of MR products, the films turned yellow/dark brown and released antioxidant compounds (inhibition ~33%) while immersed in water, which gave the films their active properties (stabilization of free radicals). These films have considerable potential as reinforced active packaging films for renewable food packaging applications.

1. Introduction

One main strategy in the implementation of a circular economy in the food industry is to find more sustainable solutions to manage leftover food wastes and by-products (Garcia-Garcia, Stone, & Rahimifard, 2019). In this matter, valorisation of remaining food by-products has been used to obtain many useful biopolymers, such as collagen/gelatin and chitin/chitosan, which can be obtained from fishing industry wastes (fish skin, bones, cartilage, ligaments, and carbs/shrimp shells, respectively), and can be used to develop green food packaging (Hosseini, Ghaderi, & Gómez-Guillén, 2021; Lopes, Antelo, Franco-Uría, Alonso, & Pérez-Martín, 2015; Tsang et al., 2019) with high transparency and excellent barrier properties against O_2, CO_2 and lipids (Cazón, Velazquez, Ramírez, & Vázquez, 2017; Etxabide, Uranga, Guerrero, & de la Caba, 2017). The demand for biodegradable and renewable materials as an alternative to synthetic and non-biodegradable petroleum-based materials is increasing. The aim is to reduce the environmental impact of current single-use packaging accumulation, which is in line with another circular economy main strategy; reduction of waste.

Gelatin, an abundant, renewable, and biodegradable protein obtained from the partial hydrolysis of collagen, has shown excellent film-forming ability, transparency, oxygen barrier and UV-light absorption (prevent photo-oxidation). Furthermore, it is a good vehicle for incorporating a wide range of additives and it possesses diverse functional groups for physical or chemical modifications. However, like some other

* Corresponding author. BIOMAT research group, University of the Basque Country (UPV/EHU), Escuela de Ingeniería de Gipuzkoa, Plaza de Europa 1, 20018, Donostia-San Sebastián, Spain.
** Corresponding author. Institute of Food Science, Technology and Nutrition (CSIC), José Antonio Novais 10, 28040, Madrid, Spain.
E-mail addresses: alaitz.etxabide@ehu.es (A. Etxabide), joaquin.gomez@csic.es (J. Gómez-Estaca).

https://doi.org/10.1016/j.lwt.2021.112833
Received 17 August 2021; Received in revised form 7 October 2021; Accepted 16 November 2021
Available online 30 November 2021

protein and polysaccharides, gelatin's high sensitivity to moisture/water, as well as poor mechanical and thermal properties, are the major disadvantages for the use of this protein as a food packaging material (Etxabide, Uranga, et al., 2017; Hosseini & Gómez-Guillén, 2018). This is especially true in the case of gelatin from cold-water fish species (Gómez-Guillén et al., 2009).

Crosslinking of gelatin has been demonstrated to be a suitable approach to overcome these drawbacks in protein-based materials. However, the selection of an appropriate crosslinker is critical. Unlike glutaraldehyde, a widely used crosslinked with toxic nature, the Maillard reaction (MR) is a natural crosslinking process that has been applied to proteins (Garavand, Rouhi, Razavi, Cacciotti, & Mohammadi, 2017). The MR is a chemical and non-enzymatic browning reaction that takes place when a protein is mixed with a sugar (reducing saccharide) at high temperatures. As a result, a large number of Maillard reaction products (MRPs), such as UV-light absorbing (prevent photo-oxidation) and dark-brown polymeric compounds, known as melanoidins, are formed (Etxabide et al., 2021).

The crosslinking strategy via the MR to enhance protein-based materials properties could also assist in improving the shelf-life of food products. This would be due to the formation of UV-light absorbing compounds (secondary antioxidant function) as well as the antioxidant activity of MRPs (primary antioxidant function) which would prevent/inhibit the oxidation reactions of lipids in foods, respectively. The enhancement of food shelf-life is in line with the current trends in the food packaging industry, which includes the development of active packaging to extend the shelf-life of food products and so, reduce food waste (Spada, Conte, & Del Nobile, 2018). Therefore, MR can be used not only to crosslink proteins but also to form natural antioxidant compounds, avoiding further use of (synthetic) additives (Nooshkam, Varidi, & Bashash, 2019; Qin et al., 2016).

Another promising way to improve biopolymer-based material properties is the inclusion of nanostructures (sizes lying in the range of 100 nm) as reinforcing fillers through the formation of nanocomposites (Ahankari, Subhedar, Bhadauria, & Dufresne, 2021; Sharma, Jafari, & Sharma, 2020). It has been shown that the addition of nanostructures into the biopolymer matrices markedly improved the mechanical, thermal, and physicochemical properties of the final nanocomposite materials (Oun & Rhim, 2017; Qin et al., 2016). Among natural nanomaterials, and unlike cellulose nanoparticles, chitin nanowhiskers (CNWs) have not been widely investigated for the development of gelatin-based food packaging materials (Ahmad & Sarbon, 2021; Sahraee, Ghanbarzadeh, Milani, & Hamishehkar, 2017; Sahraee & Milani, 2020, pp. 247–271). CNWs can be prepared from the acid hydrolysis of chitin's crystalline region from crab and shrimp shells, which are a potential natural renewable and biodegradable source of nano-sized reinforcements. CNW is a non-water soluble highly crystalline polysaccharide with high stiffness and strength. It has a large aspect ratio and specific surface area with a great number of polar hydroxyl groups on the surface, which can interact with the amino groups and carboxyl groups of protein molecules such as gelatin (Li, Cao, Pei, Liu, & Tang, 2019).

The objective of this work is to improve the functionality of gelatin films for active food packaging applications. For this purpose, a combined strategy of crosslinking via the Maillard reaction and nanoreinforcement via compounding with CNWs is examined. The thermal, mechanical, optical, structural, antioxidant and water sensitivity properties of the films were determined, as a function of CNWs addition. To the best of our knowledge, no studies have been reported on the modification of gelatin films by both the MR and the addition of CNWs for the development of reinforced and active food packaging materials.

2. Materials and methods

2.1. Materials

Type A codfish gelatin with 200 Bloom (gel strength), 11.06% moisture and 0.147% ash (Weishardt International, Liptovsky Mikulas, Slovakia) was used as a matrix to which the following additives were added: chitin from shrimp (Glentham Life Sciences (Corsham, UK)), D-(+)-glucose (Sigma Aldrich), and glycerol (ECP LabChem) as reinforcement, crosslinker and a plasticizer, respectively. HCl (ECP LabChem) was used to prepare 1 M HCl in Milli-Q water (MQW)and modify the pH of the film-forming solutions. 2,2-diphenyl-1-picryl hydrazyl (DPPH) and gallic acid were purchased from Sigma-Aldrich, while ethanol and methanol were obtained from ECP LabChem (Auckland, New Zealand).

2.2. Chitin nanowhiskers (CNWs) characterization

2.2.1. CNWs preparation

CNWs were prepared by acid hydrolysis as per Gopalan Nair & Dufresne (2003), with modifications. Ten grams of chitin was placed in a round bottom flask with 400 mL of 3 N HCl and boiled for 90 min under constant reflux. Samples were transferred to test tubes and allowed to decant overnight. Then, part of the supernatant was discarded. The concentrated whiskers suspension was diluted with distilled water, centrifuged at 36,000 rpm at 15 °C for 40 min (Sorvall Combiplus, Dupont, Wilmington, DE, USA), and then the supernatant was removed. The precipitate was dialyzed against distilled water using a 12–14,000 Da molecular weight cut membrane (Medicell Membranes Ltd, London, UK) for 3–4 days with daily water change until pH ≈ 4. The neutralized whiskers were sonicated in 200 mL aliquots for 5 min (1 min on/1 min off cycles) using a Q sonica equipment (Q700 model, Newton, CT, USA) set at 95% amplitude and in a water/ice bath to avoid overheating.

2.2.2. CNWs morphology

The structure of CNWs was evaluated by transmission electron microscopy (TEM, JEOL JEM-1230). Adequately diluted samples were analysed after being adsorbed on glow-discharged carbon-coated grids and stained with 2% uranyl acetate. Grids were observed at 100 kV and a nominal magnification of 50 K. Images were taken under low dose conditions with a CMOS Tvips TemCam-F416 camera, at 2.28 Å per pixel. The length and width of the whiskers were analysed with the Image J software after measuring more than 100 whiskers taken from 9 different photographs.

X-ray diffraction studies of CNWs (and films, n = 3) were performed with a diffraction unit (Empyrean, Malvern Panalytical, Cleveland, New Zealand) operating at 45 kV and 40 mA. The radiation was generated from a Cu-Kα ($\lambda = 1.5418$ Å) source. The diffraction data of the samples were collected from 2θ values from 5° to 50°, where θ is the incidence angle of the X-ray beam on the sample. The crystallinity index (CI) of CNWs was determined as follows (Dominic et al., 2020):

$$CI\ (\%) = \frac{(I_{110} - I_{13^\circ})}{I_{110}} \times 100 \quad (1)$$

where I_{110} is the intensity at 18.9° and I_{13° is the intensity at 13°.

2.2.3. Thermo-gravimetric (TG) and differential scanning calorimetry (DSC) analyses of CNWs

Thermo-gravimetric measurements (n = 2) were performed in a TA Instruments equipment (Q5000, Alphatec Systems Limited, Auckland, NZ). CNWs (5.0 ± 0.1 mg) were tested from 22 °C up to 500 °C at a heating rate of 10 °C/min under nitrogen atmosphere (25 mL/min) to avoid thermo-oxidative reactions. DSC measurements (n = 2) were performed using a TA Instruments system (Q1000, Alphatec Systems Limited, Auckland, NZ) equipped with an electric intercooler as a

refrigeration unit. Samples (3.5 ± 0.1 mg) were hermetically encapsulated in aluminium pans to prevent mass losing during heating from −80 to 225 °C at a rate of 10 °C/min, cooling to −80 °C at a rate of 5 °C/min and heating to 425 °C at a rate of 10 °C/min under inert atmosphere conditions (30 mL/min N_2).

2.3. Film characterization

2.3.1. Film preparation

Fish gelatin-based films with different CNW contents were prepared by casting. Amounts of 2.5 g of gelatin, 10 wt% of glucose (based on preliminary studies where film crosslinked with 10% glucose presented lower solubility values than the films containing 2.5, 5, & 7.5% glucose) and 10 wt% of glycerol (based on previous studies (Etxabide, Coma, Guerrero, Gardrat, & de la Caba, 2017; Etxabide, Uranga, Guerrero, & de la Caba, 2015)) (both on a gelatin dry weight basis) were dissolved in 40 mL Milli-Q water (MWQ) for 30 min at 60 °C under continuous stirring (250 rpm) to obtain a good blend. Then, the pH of the film-forming solution (FFS) was adjusted to 3.44 ± 0.03 with 1 N HCl (to prevent aggregation of the CNWs added later on), and the blend was maintained at 60 °C for 30 min under stirring. Meanwhile, CNW aliquots (1, 2, and 4 wt%, based on a gelatin dry weight basis) were prepared in 10 mL of MWQ and treated with an ultrasonic wave (the dispersibility process of CNWs was optimized previously (Table 1S and Fig. 1S) at 225 W for 1 min (30 s on/30 s off cycles). After that, both solutions were mixed, and the resulting mixture was stirred for an additional 10 min at 250 rpm. The final gelatin concentration on the mixture was 5% (w/v). Finally, 7.5 g of the FFS was poured into each Petri dish (ø 90 mm) and left to dry and form the film in an air-circulating fume hood at 20 °C and 56% RH for 24 h. Some samples were then peeled from the dishes and heated at 105 °C for 24 h to promote glycation. All films were conditioned at 20 °C and 63% relative humidity for a minimum of 48 h before testing. The following designation was used for naming each system as a function of heat-treatment and CNW content: No-heated films with 0 wt% CNWs as 0-NH and heat-treated films with 0, 1, 2, and 4 wt% of CNWs as 0-HT, 1-HT, 2-HT, and 4-HT, respectively.

2.3.2. Thermal characterization of films-TGA/DSC

Thermo-gravimetric measurements of films (4.0 ± 0.4 mg) were performed as described in section 2.2.3. DSC measurements were performed by heating the films (3.5 ± 0.1 mg) from −80 to 250 °C at a rate of 10 °C/min under inert atmosphere conditions (30 mL/min N_2).

2.3.3. Mechanical properties

Young's modulus (E), ultimate tensile strength (UTS) and elongation at break (EB) were measured for each film at least five times on an Instron 5943 mechanical testing system (Instron, Norwood, USA) according to ASTM D882-02 (ASTM, 2002). Samples were cut into strips of 50 mm × 10 mm, the gauge length was set to 30 mm, and the testing was carried out at 1 mm/min crosshead speed with a 50 N load cell.

2.3.4. Attenuated total reflection-Fourier transform infrared (ATR-FTIR) spectroscopy

FTIR spectra of the individual components and films were carried out on a Bruker Vertex 70 FTIR spectrometer using a single bounce Platinum Diamond Micro-ATR accessory (Bruker Optics, New Zealand) to analyse the MR and the interactions between the nanowhiskers and gelatin. A total of 32 scans were performed at 4 cm^{-1} resolution and the measurements were recorded between 4000 and 800 cm^{-1}. Normalization of each obtained spectrum was done using OPUS 7.5 software while the second derivative of the amide I absorbance band was calculated by applying a Savitzky–Golay filter (second order, 11 smoothing points) in OriginPro software (Núñez-Flores et al., 2013).

2.3.5. Structural properties

Polarized light microscopy examinations were carried out using a Leica DMR upright microscope with a Nikon Digital Sight DS-5MC-U1 cooled colour camera and Nikon NIS Elements software for image acquisition (n = 2).

2.3.6. Optical properties

Colour was determined using a Minolta CR-300 colourimeter (Konica Minolta, Japan) as per Etxabide et al. (2021). Total colour difference (ΔE*) values (n = 9) for heat-treated films as a function of CNWs concentration, were calculated referred to the control (0-NH) films (placed onto a white paper sheet) as follows:

$$\Delta E^* = \sqrt{(\Delta L^*)^2 + (\Delta a^*)^2 + (\Delta b^*)^2} \quad (2)$$

A Shimadzu UV-3600 plus spectrophotometer (Shimadzu Europa, GmbH, Germany), and the software UVProve Version 2.5, were used to assess the effect of MR and the addition of different concentrations of CNWs on the barrier properties of films to ultraviolet (UV) and visible (Vis) light at wavelengths from 200 to 800 nm. Besides, the transparency of the films was determined at 600 nm. Three specimens were tested for each composition (n = 3) and the transparency (T) was calculated as follows:

$$T = \frac{A_{600}}{x} \quad (3)$$

where A_{600} is the absorbance value at 600 nm and x is the average thickness (mm) of the films. Film thickness was measured using a digimatic micrometre (ID-H Series 543 Mitutoyo, China) and three measurements at different positions were taken on each film and 4 films were analysed (n = 12).

2.3.7. Film properties in contact with water

Water contact angle (WCA) measurements were performed using an optical contact angle measuring instrument (CAM 100, KSC instruments Ltd., Finland). A 4 μL MQW drop was placed on different sample surface regions to estimate the hydrophilic/hydrophobic character of films. The image of the drop was taken using CAM100 software after 60 s of the droplet deposition. Twelve measurements (n = 12) were taken for each composition at 20 °C and 67% RH.

For solubility measurements, three specimens (n = 3) of each film were weighed (W_o) and immersed in 10 mL of MQW at 20 °C for 24 h. After that, specimens were taken out of MWQ and left to dry in an air-circulating fume hood at room temperature (20 °C) for 24 h before reweighing (W_t). The solubility of films was calculated by the following equation:

$$Solubility\ (\%) = \frac{(W_o - W_t)}{W_o} \times 100 \quad (4)$$

The release of Maillard reaction products (MRPs) from films into MQW was analysed by immersing the films (3.5 cm^2) in 10 mL of MQW at 20 °C for 24 h. After that, specimens were taken out of MQW and the liquid was analysed by introducing the samples in quartz cuvettes at a NanoPhotometer (NP80, IMPLEN, Europe) and recording wavelengths from 200 to 400 nm (Etxabide, Coma, et al., 2017). Three films (n = 3) were analysed for each composition.

2.3.8. Antioxidant activity of films

The DPPH test is used for the assessment of the free radical scavenging potential of an antioxidant molecule and is considered one of the standard methods for the evaluation of antioxidant properties of biopolymeric antioxidant films (Khan, Di Giuseppe, Torrieri, & Sadiq, 2021). So, in this study, DPPH radical scavenging activity was measured according to the method of Etxabide, Coma, et al. (2017) on the liquid samples (n = 3) obtained after the release test. Free radical scavenging activity of samples was expressed as μg/mL gallic acid equivalent (GAE, calibration curve (0.125–1.25 μg/mL): y = 2.34 + 59.77x, R^2 0.999). The inhibition values were determined by the absorbance decrease at

517 nm as follows:

$$Inhibition\ (\%) = \frac{A_c - A_s}{A_c} \times 100 \quad (5)$$

where A_c is the absorbance of the MQW where 0-NH films were immersed and A_S is the absorbance of the MQW where HT films with different CNWs amounts were immersed.

2.4. Statistical analysis

Data were subjected to one-way analysis of variance (ANOVA) through an SPSS computer program (SPSS Statistic 25.0). Post hoc multiple comparisons were determined by Tukey's test with the level of significance set at $p < 0.05$.

3. Results and discussion

3.1. CNWs characterization

3.1.1. Morphology of CNWs

CNWs had a rod-shaped morphology (Fig. 1 a) with an average length and width of 206 ± 72 nm and 18 ± 5 nm, respectively. Similarly, Dominic et al. (2020) prepared rod-like morphology whiskers from shrimp shells with a diameter range between 25 and 32 nm and length around 400 nm. After the acid hydrolysis, the crystal structure of CNWs was confirmed (Fig. 1 b) by the presence of a very intense peak at 18.9° (1 1 0), four weaker peaks at 9.1° (0 2 0), 12.4° (0 2 1), 23.0° (1 3 0) and 26.0° (0 1 3), as well as by the crystallinity index of 90.2 ± 0.6%. Comparable XRD diffraction patterns were found in the literature, which indicated the extracted polysaccharide was α-chitin, as well as similar crystallinity indexes (around 86%) were seen in earlier research (Dominic et al., 2020; Gbenebor, Adeosun, Lawal, Jun, & Olaleye, 2017; Qin et al., 2016).

3.1.2. Thermal properties of CNWs

Thermogravimetric (TG) and derivative thermogravimetric (DTG) curves (Fig. 2 a) of the prepared CNWs revealed two main weight loss regions: i) at a temperature up to 150 °C, related to the evaporation of physically weak and chemically bound water; and ii) around 250–450 °C, associated with the thermal decomposition of CNWs. A maximum degradation temperature (T_{max}) of 379 °C was observed, which resulted in a loss of more than 45 wt% of the initial mass. The final residue at 600 °C was around 15%. Similar results have been reported in the literature (T_{max} at 332 °C with ~50% degradation, and 14% residue at 500 °C (Dominic et al., 2020)).

The DSC thermogram (Fig. 2 b) showed two characteristic peaks during heating, one endothermic and the other exothermic. The endothermic peak occurred around 65–71 °C and was attributed to the dehydration process, the release of bound water from the chitin molecules. The exothermic peak in the range of 320–325 °C was attributed to the thermal degradation of chitin. No peaks related to melting and crystallization were observed in the heating/cooling processes, respectively, reflecting the finding that polysaccharides do not melt but are thermally degraded (Rodrigues et al., 2020).

3.2. Film characterization

3.2.1. Thermal properties of films

TGA thermograms (Fig. 3 a & b) show that all films presented similar behaviour with three weight loss stages: i) up to 150 °C was related to the loss of free and absorbed water; ii) up to 220 °C, was associated with the loss of low molecular weight protein fractions, plasticizer and structurally bonded water; and iii) up to 420 °C was related to the degradation of large size gelatin fractions. Unlike the heat-treatment and the addition of 1 and 2 wt% CNWs, the incorporation of 4 wt% CNWs increased the degradation temperature of gelatin films when compared to control samples (Table 1) since the peak of maximum degradation temperature shifted 5 °C from 0-NH to 4-HT films. This could be related to the modification of gelatin structure by the incorporation of CNWs, which could i) change the crystallinity of the gelatin matrix due to its crystalline nature (Fig. 1b) and ii) promote new interaction between the polar hydroxyl groups in chitin with the amino groups and carboxyl groups of gelatin (Li et al., 2019). These modifications could require higher thermal energy for dissociating the crystals and breaking the interactions, resulting in more thermally stable films (George & Siddaramaiah, 2012; Sahraee et al., 2017; Wang et al., 2013).

DSC thermograms (Fig. 3 c) of gelatin films showed two endothermic peaks, one around 70 °C, related to the random coil region of gelatin (George & Siddaramaiah, 2012) and another around 160 °C associated with the melting temperature of glucose (Wang, Truong, Li, & Bhandari, 2019). When films were heated (0-HT), an increase in temperature of both endothermic peaks was observed (Table 1), indicating that the

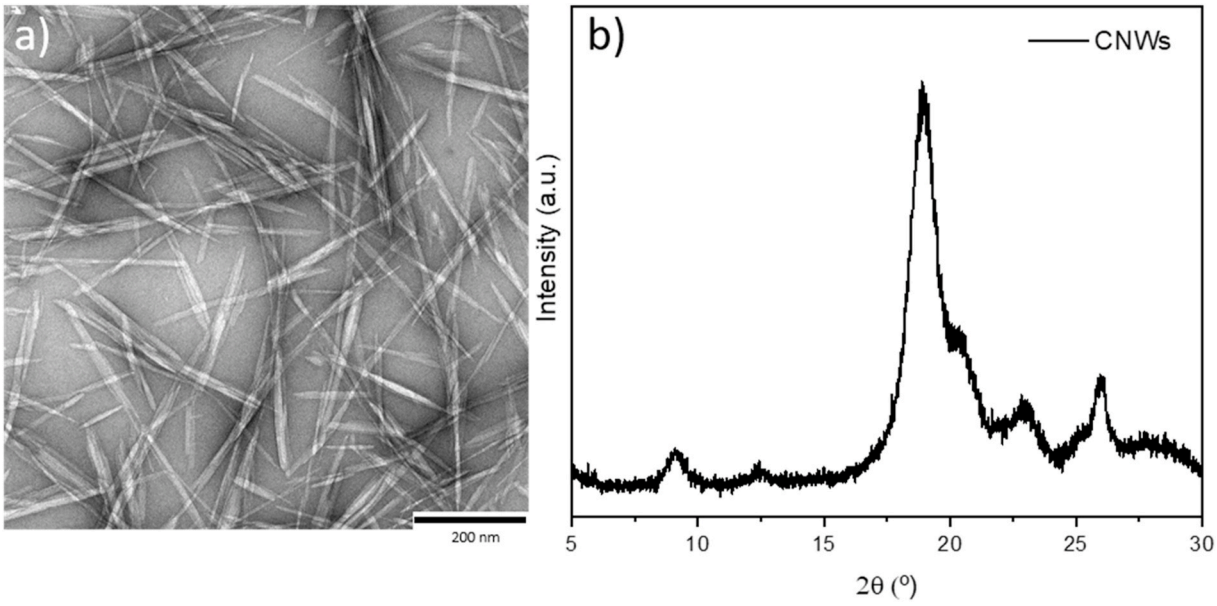

Fig. 1. a) TEM image and b) XRD pattern of chitin nanowhiskers (CNWs) prepared from shrimp chitin (n = 3).

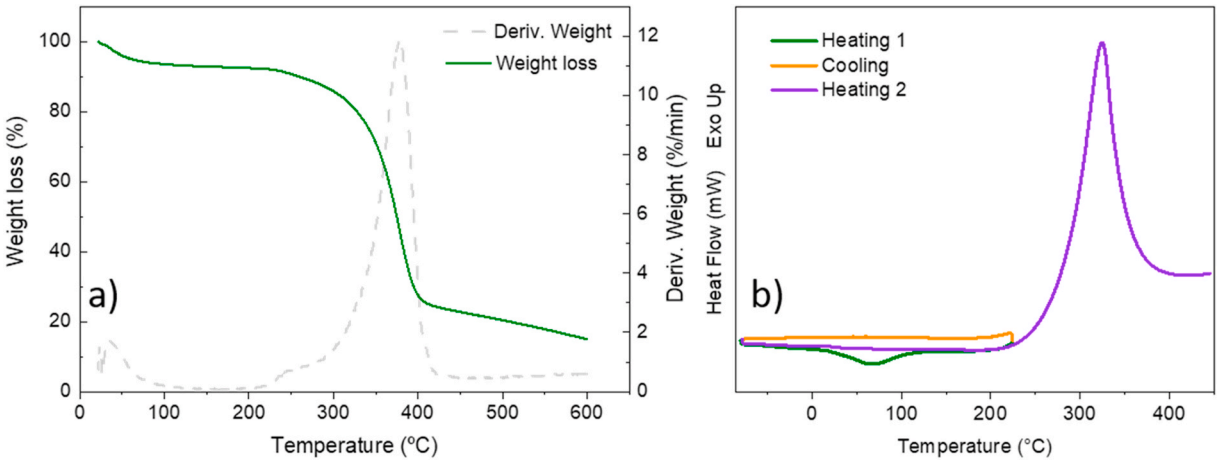

Fig. 2. a) TGA and TGA derivative (Deriv.), and b) DSC thermogram (heating 1 up to 225 °C, cooling up to −80 °C, and heating 2 up to 450 °C) of chitin nanowhiskers under N_2 atmosphere conditions (n = 2).

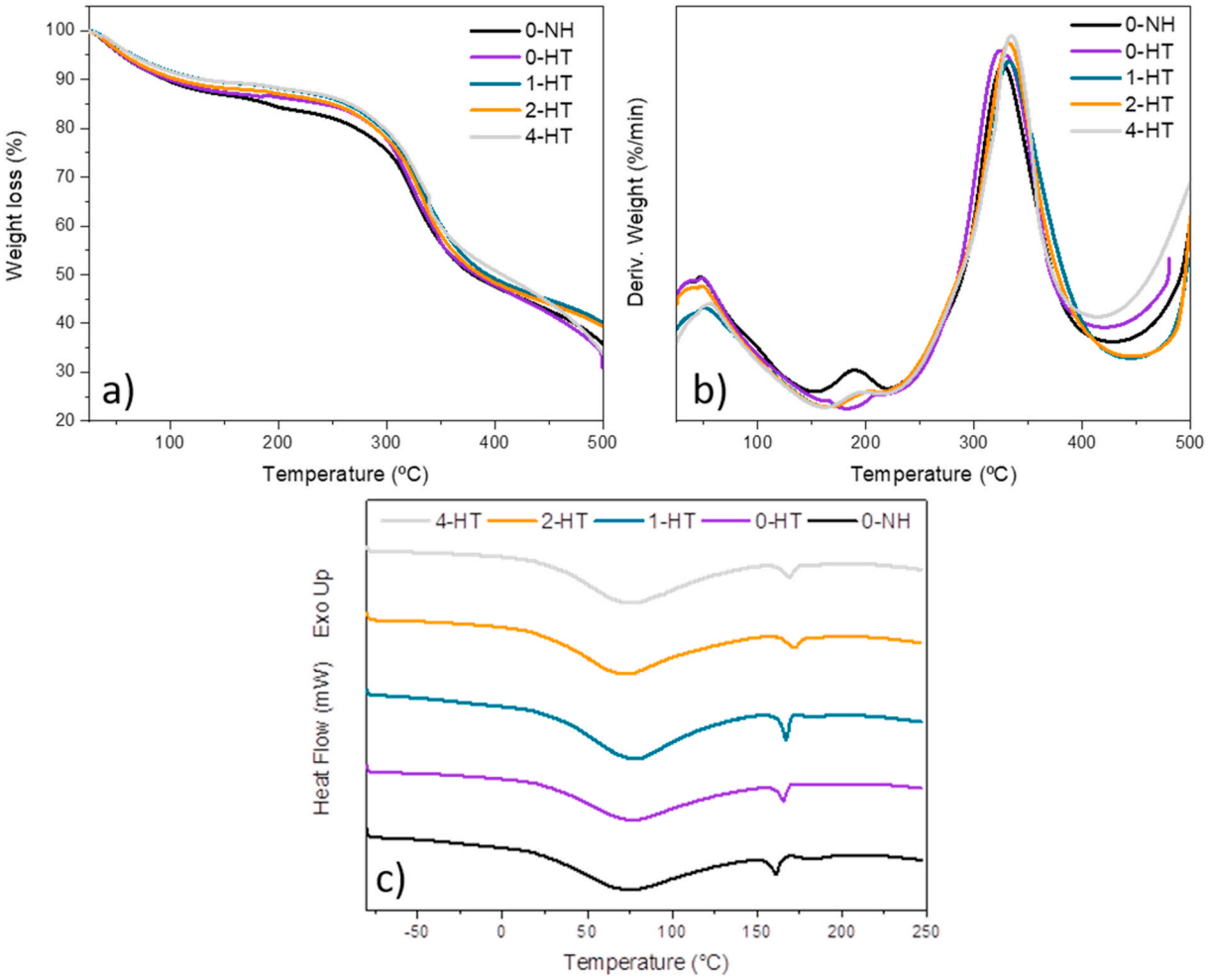

Fig. 3. a) TGA, b) TGA derivative (Deriv.), and c) DSC thermograms of gelatin films as a function of chitin nanowhiskers concentration (0, 1, 2, & 4 wt% on a gelatin dry weight basis) and heat-treatment (non-heated (NH); heat-treated (HT)) (n = 2).

crosslinking of gelatin with glucose thermally stabilized the gelatin matrix. A higher increment in temperatures was observed when CNWs were added. The 4-HT films showed higher shiftiness in both endothermic peak temperatures, which indicated a further stabilization of gelatin matrix with the addition of CNWs. These results could be related to the new covalent crosslinking via MR and noncovalent (electrostatic interactions and hydrogen bonding) interactions between glucose and CNWs with gelatin, as well as changes in crystallinity of the films due to the presence of crystalline CNWs (George & Siddaramaiah, 2012; Kchaou et al., 2018; Sahraee et al., 2017; Wang et al., 2013).

Table 1
Degradation temperature (T_d) of gelatin films analysed using TGA; temperature T_1 related to random coil region of gelatin and temperature T_2 related to glucose melting analysed using DSC (n = 2); and Young's modulus (E), ultimate tensile strength (UTS) and elongation at break (EB) values (n = 5) of non-heated (NH) and heat-treated (HT) gelatin films containing different concentrations of chitin nanowhiskers (0, 1, 2 & 4 wt%, on a gelatin dry weight basis). Two means followed by the same letter in the same column are not significantly ($P > 0.05$) different through Tukey's multiple range test.

Films	TGA/DTGA	DSC		Mechanical properties		
	T_d (°C)	T_1 (°C)	T_2 (°C)	E (MPa)	UTS (MPa)	EB (%)
0-NH	328.5 ± 1.8	71.7 ± 2.8	160.7 ± 0.6	1476 ± 78^{a}	42.2 ± 2.0^{a}	16.9 ± 1.4^{a}
0-HT	327.2 ± 1.3	75.8 ± 0.3	165.6 ± 0.1	2455 ± 74^{b}	71.0 ± 1.8^{b}	7.7 ± 0.5^{bc}
1-HT	331.1 ± 1.5	76.7 ± 0.3	166.9 ± 0.3	2435 ± 50^{b}	69.5 ± 2.0^{b}	7.8 ± 0.6^{bc}
2-HT	331.5 ± 1.5	75.3 ± 2.6	169.5 ± 2.4	2496 ± 56^{b}	68.9 ± 3.3^{b}	9.1 ± 1.2^{b}
4-HT	333.5 ± 1.6	75.5 ± 0.9	169.2 ± 0.0	2921 ± 76^{c}	77.4 ± 3.1^{c}	6.8 ± 1.1^{c}

3.2.2. Mechanical properties of films

Control films (0-NH) showed values (Table 1) of Young's modulus (E), ultimate tensile strength (UTS) and elongation at break (EB) of 1476 ± 78 MPa, 42 ± 2 MPa, and 17 ± 1%, respectively. It is worth mentioning that along with glycerol, the non-reacted glucose could act as a plasticizer in 0-NH films as observed by Kchaou et al. (2018) where the EB increased by 54% in gelatin films after glucose addition. However, the heating of films promoted the MR, formation of chemical crosslinks, which notably increased the E and UTS values (by ~66%) while EB values decreased (by ~54%). Similar trends were found in the literature (Kchaou et al., 2018) where glucose-crosslinked gelatin films presented better tensile strength (TS) and E. The enhancement was related to the crosslinking via MR.

The addition of CNWs presented the same trend (E and UTS increase by 18 and 8%, respectively, and EB decreased by 11% for 4-HT films in comparison to the 0-HT films), and the effect was greater as their concentration increased. Changes in mechanical properties with the addition of CNWs could be connected to both the reinforcing effect of homogeneously dispersed CNWs due to their stiffness, strength and crystallinity, as well as the formation of noncovalent interaction such as hydrogen bonding between CNWs and gelatin. Similar results were found in the literature (Shankar, Reddy, Rhim, & Kim, 2015), where the TS and E values of carrageenan/chitin nanofibrils films increased (by ~50%) while the EB decreased (by ~48%) with an increase in the chitin concentration from 0 to 5%. These alterations were related to the chitin nanostructure's high stiffness and strength as well as the formation of hydrogen bonding forces.

3.2.3. Interactions between components

In the analysis of individual components (Fig. 2S), the main absorption bands of gelatin were related to N–H stretching at 3290 cm^{-1} (amide A), C═O stretching at 1630 cm^{-1} (amide I), N–H bending at 1545 cm^{-1} (amide II) and C–N stretching at 1239 cm^{-1} (amide III) (Barth, 2007). The main absorption bands of glycerol were related to the five bands corresponding to the vibrations of C–C bonds at 850, 920 and 980 cm^{-1} and C–O bonds at 1350 and 1110 cm^{-1} (Liu et al., 2017). The bands associated with glucose were at 836 cm^{-1} (C–C stretching), 914 and 992 cm^{-1} (C–CH and C–CO stretching), 1017, 1047, and 1105 cm^{-1} (C–C and C–O stretching and C–CH bending), and 1144 cm^{-1} (C–O and C–C stretching) (Wiercigroch et al., 2017). The main absorption bans of CNWs were related to O–H stretching at 3438 cm^{-1}, amide I (C═O) at 1619 cm^{-1}, amide II (N–H bending and C–N stretching) at 1553 cm^{-1}, amide III (CH_2 wagging) at 1308 cm^{-1}, and the five bands (1154, 1114, 1070, 1010, and 952 cm^{-1}) related to oxygen stretching, ring stretching, C–O–C stretching in the ring, C–O stretching in the ring and CH_3 wagging, respectively. It was observed that the amide I band was divided into two sharp peaks, 1655 and 1619 cm^{-1}, confirming its status as α-chitin (Kaya et al., 2017), as seen in XRD results (Fig. 1 b).

In the analysis of films (Fig. 4 and Table 2S), small shifts of amide II, amide III and saccharide bands were observed when films without CNWs were heated (0-HT) (Fig. 4 a). These alterations have been related in the literature (Kchaou et al., 2018) to the structural changes that occurred during the crosslinking reaction between gelatin and glucose (Fig. 4S). Furthermore, a merge of the two bands situated in the saccharide region (1150-900 cm^{-1}) could also be seen, which was related to the consumption of saccharides during the MR (Etxabide et al., 2021). The addition of CNWs into the gelatin films (Fig. 4 b) showed no significant changes in the FTIR spectra of the films since low relative molecular masses of CNWs molecules could lead to relatively weak absorption bands, as compared to those of the gelatin molecules. However, the bands associated with amide II, amide III and saccharide region slightly shifted to lower wavenumbers, comparing to 0-HT films (Table 2S). These outcomes could be related to hydrogen bonding between the hydroxyl groups of CNWs and the amino groups of gelatin, as well as electrostatic interaction between amino groups of CNWs and carboxyl groups of gelatin (Fig. 4S) (Garrido, Etxabide, de la Caba, & Guerrero, 2017; Qiao, Ma, Zhang, & Yao, 2017). These interactions in films were further analysed by assessing the secondary derivative of the amide I band (Fig. 3S). The heating and the addition of CNWs induced significant changes in the secondary structure of gelatin, as seen in the variations of the band centred at 1654 cm^{-1}. This has been related to the hydrogen bonding interferences in the triple helical component of the gelatin, as analysed by Núñez-Flores et al. (2013).

3.2.4. Structural properties

XRD results of all gelatin films (Fig. 5) displayed two diffraction peaks: a sharp peak at 7.5°, corresponding to the residual triple-helix from native collagen, and a broad peak at 20°, related to the partial crystalline structure of fish gelatin (Liu, Antoniou, Li, Ma, & Zhong, 2015). Unlike the heat-treatment of films, the addition of CNWs induced changes in XRD diffraction patterns of gelatin films, since new peaks at around 9° and 19° were seen, typical of a highly crystalline structure of CNWs previously observed in Fig. 1 b. The intensity of the peaks was more pronounced with an increase in CNWs content. Similar results were observed in maize starch/chitin nanofibrils nanocomposite films with the addition of 0–5 wt% chitin (Qin et al., 2016) where the introduction of higher CNWs content (up to 5%) significantly increased the magnitude of the diffraction peaks at 9.2° and 19.1°. The authors indicated that the increase in crystallinity of the maize starch/chitin CNWs films was due to the higher concentrations of crystalline CNWs in the polymer matrix.

The changes in crystallinity observed by XRD were further analysed by a polarized light optical microscope (Fig. 6). In 0-NH films, glucose crystals were observed since sugars tend to crystalize while drying. When the films were heat-treated (0-HT) the presence of crystals reduced due to glucose was consumed in the MR, as seen in the FTIR results (Fig. 4, merge of the two bands situated in the saccharide region). The addition of CNWs notably modified the morphology of the samples and rougher structures were seen as their content increased. Although CNW crystals were barely visible due to gelatin embedded them within the matrix, some crystals could be seen in the samples with high CNWs concentration (4-HT). These micrographs also showed that CNWs were dispersed homogeneously on the gelatin matrixes (Haghighi et al., 2021).

These and FTIR results indicated that changes in crystallinity in films might be the main cause of the observed changes in thermal and mechanical properties of films, while the noncovalent interactions between gelatin and chitin could contribute, to a lesser extent, to alter these properties.

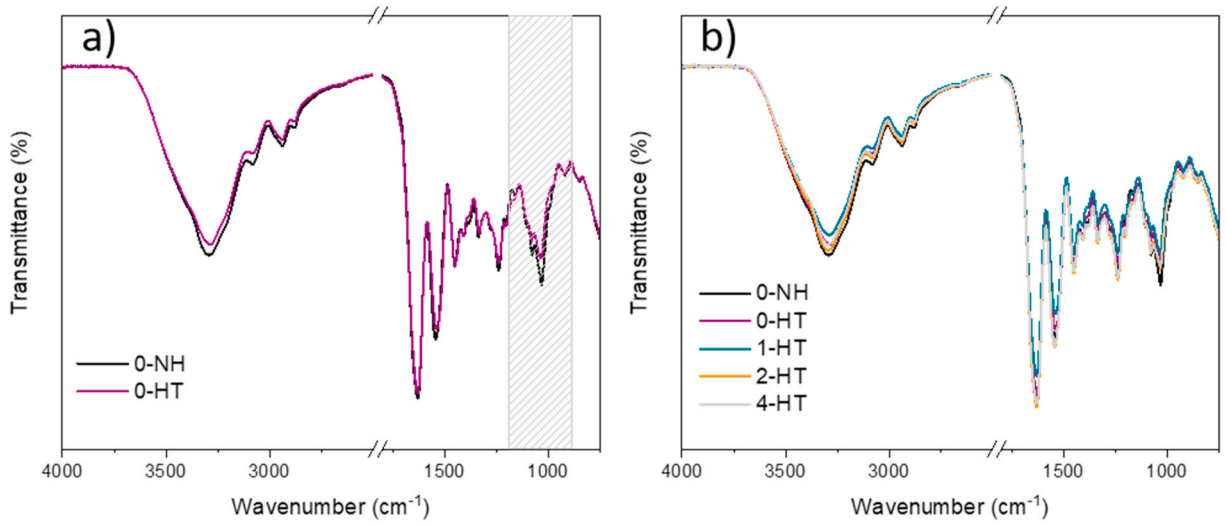

Fig. 4. FTIR spectra of a) non-heated (NH) and heat-treated (HT) gelatin films, b) containing different concentrations of chitin nanowhiskers (0, 1, 2, & 4 wt% on a gelatin dry weight basis) (n = 3).

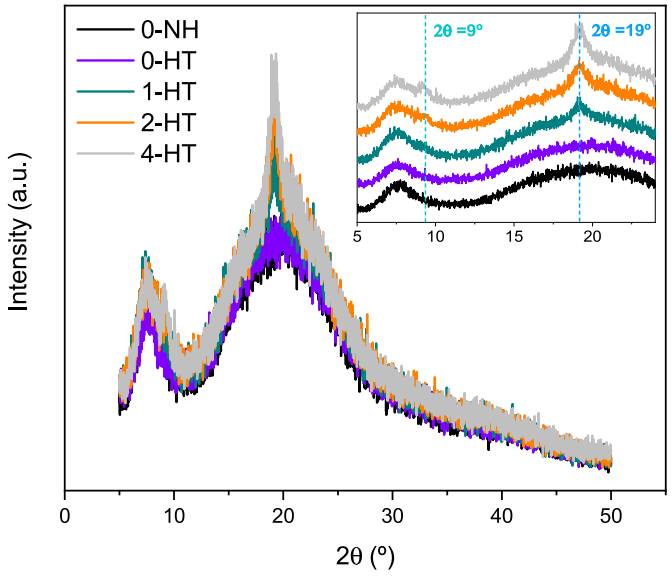

Fig. 5. XRD patterns of non-heated (NH) and heat-treated (HT) gelatin films containing different concentrations of chitin nanowhiskers (0, 1, 2, & 4 wt% on a gelatin dry weight basis) (n = 3).

3.2.5. Optical properties

Films were 45.4 ± 4.0 μm thick and no significant differences were seen with heating and CNW additions in the thickness. However, the heating process significantly affected the colour properties of the films (Table 2 and Fig. 5S), since the uncoloured films (0-NH) turned to yellow and dark brown with the heat-treatment (HT). This was due to the presence of glucose and gelatin within the films, which promoted MR and the formation of melanoidins, dark-brown polymeric compounds (Etxabide et al., 2021) while the heating of films. The addition of CNWs did not have any effect on the colour parameters of the films, irrespective of their concentrations. The transparency of films (Table 2 and Fig. 5S), however, was notably affected, since both MR and the addition of CNWs decreased the light transmission capacity of films, resulting in lower light transmittance as the presence of CNWs increased. The reduction of light transmittance after MR was related to the formation of MRPs, which can absorb light in the visible spectrum (Etxabide et al., 2021). Regarding CNWs, the presence of crystalline regions could induce light scattering in films, resulting in less transparent (reduction by 31%) films (Wang et al., 2018). Similar trends were found in the literature (Shankar et al., 2015), where the addition of 0–5% chitin nanofibrils linearly decreased the light transmittance (by ~5%) in carrageenan/chitin nanofibrils films. However, all films were considered transparent since similar or lower T values than commercial films, such as oriented polypropylene (1.57) and low-density polyethene (4.26) films (Guerrero, Stefani, Ruseckaite, & de la Caba, 2011), were obtained.

Regarding light barrier properties of films (Fig. 7), gelatin films (0-NH) exhibited high protection against UV light from 200 to 300 nm related to the presence of COOH, $CONH_2$ and C═O groups in polypeptide chains, and the peptide bonds of codfish gelatin (200–250 nm), as well as chromophores such as tyrosine and phenylalanine (250–300 nm), common aromatic amino acids found in proteins (Bonilla & Sobral, 2016). The heat-treatment considerably improved the UV–vis absorption capacity of films (0-HT). This light absorption enhancement was related to MR. The increase in absorbance in the UV region (λ_{max} 294 nm) provided films with a preventive (secondary) antioxidant function (by reducing the occurrence of photo-oxidation reactions in foods) (Vilela et al., 2018). This is due to the formation of uncoloured compounds in MR, precursors for the formation of melanoidins (brown and non-soluble compounds), which are mainly detected at 420 nm (visible region), and are responsible for the colouration of the films (Etxabide et al., 2021). The addition of CNWs did not significantly affect the UV–Vis absorption capacity of films (Fig. 7 b), or the extension/progression of the MR, irrespective of CNW concentrations.

3.2.6. Film properties in contact with water

WCA and solubility of films were measured (Table 3) to study the effect of MR and nanowhiskers addition on gelatin film properties when in contact with water. Control samples (0-NH) were hydrophilic (WCA <90°) films and the heat-treatment (0-HT) notably reduced the hydrophilicity of films, as the addition of CNWs had only a minor effect. The reduction of surface wettability could be related to the formation of chemical crosslinks during the MR as well as changes in film crystallinity and the formation of interactions between CNWs and gelatin. These interactions and the presence of crystalline regions could produce changes in protein structure, as shown in XRD, optical microscope, and FTIR analysis and reported in the literature (Etxabide et al., 2015; Garrido et al., 2017), which altered the wettability of films.

Regarding the solubility, it was seen that the 0-NH films were swollen to a large extent and lost their physical integrity after water immersion, and were broken into small pieces when they were taken out

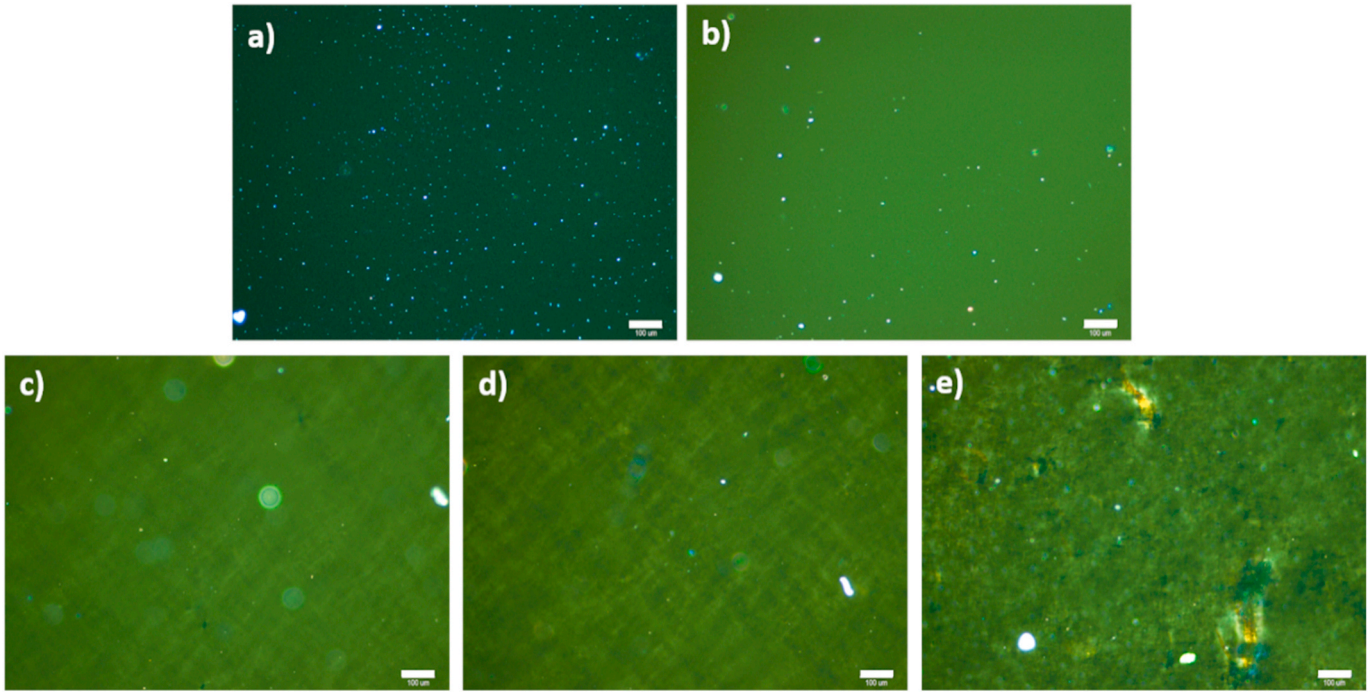

Fig. 6. Polarized light optical micrographs of a) non-heated (NH) and b)-e) heat-treated (HT) gelatin films containing different concentrations of chitin nanowhiskers (0, 1, 2, & 4 wt% on a gelatin dry weight basis). Magnification ×10 (n = 2) (scale bar 100 μ).

Table 2
Thickness (n = 13), colour parameters (L*, a*, b* and ΔE, n = 9), and transparency (T) values (n = 3) of non-heated (NH) and heat-treated (HT) gelatin films containing different concentrations of chitin nanowhiskers (0, 1, 2 & 4 wt %, on a gelatin dry weight basis). Two means followed by the same letter in the same column are not significantly (P > 0.05) different through Tukey's multiple range test.

Films	Thickness (μm)	L*	a*	b*	ΔE	T
0-NH	43.5 ± 4.3^{a}	90.32 ± 0.06^{a}	6.94 ± 0.02^{a}	−10.53 ± 0.02^{a}	–	0.91 ± 0.06^{a}
0-HT	46.0 ± 3.7^{a}	79.93 ± 0.67^{b}	8.26 ± 0.70^{b}	32.47 ± 1.00^{b}	44.27 ± 1.13^{a}	1.39 ± 0.07^{b}
1-HT	46.5 ± 3.5^{a}	79.57 ± 0.14^{b}	8.68 ± 0.14^{b}	32.67 ± 0.22^{b}	44.56 ± 0.23^{a}	1.77 ± 0.14^{bc}
2-HT	46.6 ± 4.1^{a}	79.33 ± 0.21^{b}	8.60 ± 0.18^{b}	33.30 ± 0.76^{b}	45.22 ± 0.79^{a}	1.90 ± 0.23^{c}
4-HT	44.5 ± 3.4^{a}	79.37 ± 0.19^{b}	8.50 ± 0.17^{b}	32.62 ± 0.90^{b}	44.55 ± 0.92^{a}	2.03 ± 0.08^{c}

from the MQW. However, the heating of samples (0-HT) notably maintained the physical integrity of films and significantly decreased (by ~87%) their solubility up to 13% ± 1, due to the formation of crosslinks via MR. In this context, Kchaou et al. (2018) reported that the solubility of glucose-crosslinked gelatin films decreased about 80% after 24 h of heating at 90 °C, compared to the control films (without glucose). The solubility reduction was related to the covalent bonds formed during MR which induced a decrease of water solubility in the films. A further decrease (by ~22%) was observed with the presence of CNWs, especially at 2 and 4 wt%, which was related to the increase in non-water-soluble nanocomponent (CNWs themselves) as well as the formation of noncovalent interactions between the protein and CNWs, as reported in the literature (Garrido et al., 2017; Qin et al., 2016). WCA and solubility results showed that the irreversible crosslinking induced via MR and the addition of CNWs could be used to increase the water stability of protein-based systems for food packaging applications.

3.2.7. *Antioxidant properties of films*

During film immersion in MQW, different compounds present in the films (gelatin, glycerol, glucose, CNWs, MRPs) could migrate from the sample into the liquid. Therefore, the release of compounds from films into MWQ was studied (Fig. 6S). The crosslinking reduced the release of gelatin since a narrowing in the absorption band of gelatin was observed, after the heat-treatment (0-TH). The crosslinking also induced the release of MPRs (bands centred at 289 nm) (Etxabide, Coma, et al., 2017) which was not affected by the increase in CNW concentration (Fig. 5S and Table 3). As water-soluble MRPs have been reported to have antioxidant activity (Yilmaz & Toledo, 2005), the antioxidant properties of the released MRPs were assessed (Table 3). HT films showed inhibition of ~33%, equivalent to ~0.53 μg/mL gallic acid. In this matter, Kchaou et al. (2018) reported that glucose-crosslinked gelatin films induced the formation of MRPs with the ability to donate hydrogen atoms, and thus to stabilize the free radicals during the DPPH radical scavenging assay. However, the addition of CNWs did not have a significant effect on the antioxidant properties of films, irrespective of their concentration. Therefore, it can be said that MR provided films with active function due to i) the increase in absorbance in the UV region (preventive (secondary) antioxidant function), and ii) the primary antioxidant function of antioxidant compounds (MRPs) formed during MR and released from films into MQW.

4. Conclusions

In the present study, crosslinking via MR and nano-reinforcement by compounding with CNWs were employed as combined strategies to improve the performance of cold fish gelatin films for food packaging applications. Chitin nanowhiskers (CNWs) with a rod-shaped morphology and high crystallinity were prepared and added in different concentrations to the formulation of cod-skin gelatin films that were subsequently thermally treated to promote Maillard reaction (MR). As a result, films improved their thermal stability, Young's modulus (from 1476 to 2921 MPa), ultimate tensile strength (from 42 to 77 MPa), water sensitivity (from 77 to 81°) properties, primary antioxidant properties (from 0 to 33% inhibition) and barrier to UV light (secondary

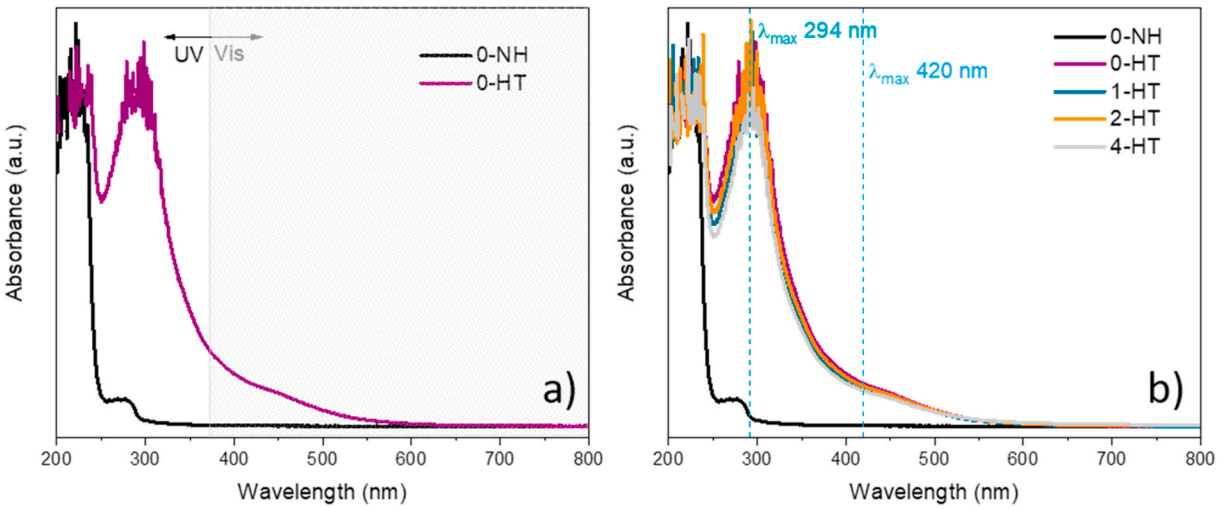

Fig. 7. UV–Vis spectra for a) non-heated (NH) and heat-treated (HT) gelatin films, b) containing different concentrations of chitin nanowhiskers (0, 1, 2 & 4 wt%, on a gelatin dry weight basis) (n = 3).

Table 3
Water contact angle (WCA) and solubility of films after immersion in Milli-Q water (MQW), absorbance values at 289 nm, inhibition, and gallic acid equivalent (GAE) of compounds released into MQW for non-heated (NH) and heat-treated (HT) gelatin films containing different concentrations of chitin nanowhiskers (0, 1, 2 & 4 wt%, on a gelatin dry weight basis). Two means followed by the same letter in the same column are not significantly (P > 0.05) different through Tukey's multiple range test. (n = 3).

			Release-DPPH		
Films	WCA (°)	Solubility	Absorbance (289 nm)	Inhibition (%)	GAE (μg/mL)
0-NH	77.3 ± 4.7^{a}	–*	0.14 ± 0.03^{a}	–	–
0-HT	80.4 ± 4.5^{abc}	13.1 ± 1.2^{a}	0.42 ± 0.01^{b}	32.6 ± 2.0^{a}	0.51 ± 0.03^{a}
1-HT	83.8 ± 2.3^{c}	12.0 ± 0.3^{ab}	0.45 ± 0.03^{b}	33.9 ± 3.3^{a}	0.53 ± 0.05^{a}
2-HT	82.8 ± 3.0^{bc}	11.0 ± 0.3^{b}	0.44 ± 0.03^{b}	35.7 ± 3.4^{a}	0.56 ± 0.06^{a}
4-HT	79.2 ± 2.0^{ab}	10.2 ± 0.2^{b}	0.41 ± 0.03^{b}	33.8 ± 1.8^{a}	0.53 ± 0.03^{a}

*Films were not dissolved but got broken into small pieces when taken out of the solution.

antioxidant action). However, the film colour shifted from uncoloured to yellow-light brown and transparency was slightly reduced, as well as the elongation at break (from 17 to 7%). FTIR and XRD analyses pointed to crosslinking via MR and changes of films' crystallinity due to the presence of CNWs as the main causes for these improvements, although the establishment of noncovalent interactions among gelatin chains and CNWs may also play a role. This study shows that crosslinking via MR and nano-reinforcement via CNWs compounding are feasible strategies to be applied in combination to improve gelatin film functionality for renewable and active food packaging materials development.

Declaration of interests

The authors declare that they have no known competing financial interests or personal relationships that could have appeared to influence the work reported in this paper.

CRediT authorship contribution statement

Alaitz Etxabide: Conceptualization, Methodology, Validation, Formal analysis, Investigation, Writing – original draft, Writing – review & editing, Visualization. **Paul A. Kilmartin:** Validation, Writing – review & editing, Funding acquisition. **Juan I. Maté:** Validation, Writing – review & editing, Funding acquisition. **Joaquín Gómez-Estaca:** Conceptualization, Methodology, Validation, Investigation, Writing – review & editing, Supervision, Funding acquisition.

Acknowledgement

The authors would like to thank the Ministry of Business, Innovation and Employment of New Zealand (MBIE, Biocide Toolbox programme) and the Spanish Ministry of Science and Innovation (projects PID2019-108361RB-I00 and AGL2017-84161-C2-1-R) for funding. A.E. thanks the State Research Agency of Spain within the Juan de la Cierva - Incorporation action (IJC2019-039697I).

Appendix A. Supplementary data

Supplementary data to this article can be found online at https://doi.org/10.1016/j.lwt.2021.112833.

References

Ahankari, S. S., Subhedar, A., Bhadauria, S., & Dufresne, A. (2021). Nanocellulose in food packaging: A review. *Carbohydrate Polymers, 255*, 117479. https://doi.org/10.1016/j.carbpol.2020.117479

Ahmad, A. A., & Sarbon, N. M. (2021). A comparative study: Physical, mechanical and antibacterial properties of bio-composite gelatin films as influenced by chitosan and zinc oxide nanoparticles incorporation. *Food Bioscience, 43*, 101250. https://doi.org/10.1016/j.fbio.2021.101250

ASTM. (2002). *ASTM d882-02 standard test method for tensile properties of thin plastic sheeting*.

Barth, A. (2007). Infrared spectroscopy of proteins. *Biochimica et Biophysica Acta (BBA) - Bioenergetics, 1767*, 1073–1101. https://doi.org/10.1016/j.bbabio.2007.06.004

Bonilla, J., & Sobral, P. J. A. (2016). Investigation of the physicochemical, antimicrobial and antioxidant properties of gelatin-chitosan edible film mixed with plant ethanolic extracts. *Food Bioscience, 16*, 17–25. https://doi.org/10.1016/j.fbio.2016.07.003

Cazón, P., Velazquez, G., Ramírez, J. A., & Vázquez, M. (2017). Polysaccharide-based films and coatings for food packaging: A review. *Food Hydrocolloids, 68*, 136–148. https://doi.org/10.1016/j.foodhyd.2016.09.009

Dominic, C. D. M., Joseph, R., Begum, P. M. S., Raghunandanan, A., Vackkachan, N. T., Padmanabhan, D., et al. (2020). Chitin nanowhiskers from shrimp shell waste as green filler in acrylonitrile-butadiene rubber: Processing and performance properties. *Carbohydrate Polymers, 245*, 116505. https://doi.org/10.1016/j.carbpol.2020.116505

Etxabide, A., Coma, V., Guerrero, P., Gardrat, C., & de la Caba, K. (2017). Effect of cross-linking in surface properties and antioxidant activity of gelatin films incorporated with a curcumin derivative. *Food Hydrocolloids, 66*, 168–175. https://doi.org/10.1016/j.foodhyd.2016.11.036

Etxabide, A., Kilmartin, P., Maté, J., Prabakar, S., Brimble, M., & Naffa, R. (2021). Analysis of advanced glycation end products in ribose-, glucose-and lactose-crosslinked gelatin to correlate the physical changes induced by Maillard reaction in films. *Food Hydrocolloids, 117*, 106736. https://doi.org/10.1016/j.foodhyd.2021.106736

Etxabide, A., Uranga, J., Guerrero, P., & de la Caba, K. (2015). Improvement of barrier properties of fish gelatin films promoted by gelatin glycation with lactose at high temperatures. *LWT-Food Science and Technology, 63*, 315–321. https://doi.org/10.1016/j.lwt.2015.03.079

Etxabide, A., Uranga, J., Guerrero, P., & de la Caba, K. (2017). Development of active gelatin films by means of valorisation of food processing waste: A review. *Food Hydrocolloids, 68*, 192–198. https://doi.org/10.1016/j.foodhyd.2016.08.021

Garavand, F., Rouhi, M., Razavi, S. H., Cacciotti, I., & Mohammadi, R. (2017). Improving the integrity of natural biopolymer films used in food packaging by crosslinking approach: A review. *International Journal of Biological Macromolecules, 104*, 687–707. https://doi.org/10.1016/j.ijbiomac.2017.06.093

Garcia-Garcia, G., Stone, J., & Rahimifard, S. (2019). Opportunities for waste valorisation in the food industry – a case study with four UK food manufacturers. *Journal of Cleaner Production, 211*, 1339–1356. https://doi.org/10.1016/j.jclepro.2018.11.269

Garrido, T., Etxabide, A., de la Caba, K., & Guerrero, P. (2017). Versatile soy protein films and hydrogels by the incorporation of β-chitin from squid pens (Loligo sp.). *Green Chemistry, 19*, 2923. https://doi.org/10.1039/C7GC02982A

Gbenebor, O. P., Adeosun, S. O., Lawal, G. I., Jun, S., & Olaleye, S. A. (2017). Acetylation, crystalline and morphological properties of structural polysaccharide from shrimp exoskeleton. *Engineering Science and Technology, an International Journal, 20*, 1155–1165. https://doi.org/10.1016/j.jestch.2017.05.002

George, J., & Siddaramaiah. (2012). High performance edible nanocomposite films containing bacterial cellulose nanocrystals. *Carbohydrate Polymers, 87*, 2031–2037. https://doi.org/10.1016/j.carbpol.2011.10.019

Gómez-Guillén, M. C., Pérez-Mateos, M., Gómez-Estaca, J., López-Caballero, E., Giménez, B., & Montero, P. (2009). Fish gelatin : A renewable material for developing active biodegradable films. *Trends in Food Science & Technology, 20*, 3–16. https://doi.org/10.1016/j.tifs.2008.10.002

Gopalan Nair, K., & Dufresne, A. (2003). Crab shell chitin whisker reinforced natural rubber nanocomposites. 1. Processing and swelling behavior. *Biomacromolecules, 4*, 657–665. https://doi.org/10.1021/bm020127b

Guerrero, P., Stefani, P. M., Ruseckaite, R. A., & de la Caba, K. (2011). Functional properties of films based on soy protein isolate and gelatin processed by compression molding. *Journal of Food Engineering, 105*, 65–72. https://doi.org/10.1016/j.jfoodeng.2011.02.003

Haghighi, H., Gullo, M., La China, S., Pfeifer, F., Siesler, H. W., Licciardello, F., et al. (2021). Characterization of bio-nanocomposite films based on gelatin/polyvinyl alcohol blend reinforced with bacterial cellulose nanowhiskers for food packaging applications. *Food Hydrocolloids, 113*, 106454. https://doi.org/10.1016/j.foodhyd.2020.106454

Hosseini, S. F., Ghaderi, J., & Gómez-Guillén, M. C. (2021). trans-Cinnamaldehyde-doped quadripartite biopolymeric films: Rheological behavior of film-forming solutions and biofunctional performance of films. *Food Hydrocolloids, 112*, 106339. https://doi.org/10.1016/j.foodhyd.2020.106339

Hosseini, S. F., & Gómez-Guillén, M. C. (2018). A state-of-the-art review on the elaboration of fish gelatin as bioactive packaging: Special emphasis on nanotechnology-based approaches. *Trends in Food Science & Technology, 79*, 125–135. https://doi.org/10.1016/j.tifs.2018.07.022

Kaya, M., Mujtaba, M., Ehrlich, H., Salaberria, A., Baran, T., Amemiya, C. T., et al. (2017). On chemistry of γ-chitin. *Carbohydrate Polymers, 176*, 177–186. https://doi.org/10.1016/j.carbpol.2017.08.076

Kchaou, H., Benbettaïeb, N., Jridi, M., Abdelhedi, O., Karbowiak, T., Brachais, C. H., et al. (2018). Enhancement of structural, functional and antioxidant properties of fish gelatin films using Maillard reactions. *Food Hydrocolloids, 83*, 326–339. https://doi.org/10.1016/j.fd.2018.05.011

Khan, M. R., Di Giuseppe, F. A., Torrieri, E., & Sadiq, M. B. (2021). Recent advances in biopolymeric antioxidant films and coatings for preservation of nutritional quality of minimally processed fruits and vegetables. *Food Packaging and Shelf Life, 30*, 100752. https://doi.org/10.1016/j.fpsl.2021.100752

Li, Y., Cao, C., Pei, Y., Liu, X., & Tang, K. (2019). Preparation and properties of microfibrillated chitin/gelatin composites. *International Journal of Biological Macromolecules, 130*, 715–719. https://doi.org/10.1016/j.ijbiomac.2019.03.014

Liu, F., Antoniou, J., Li, Y., Ma, J., & Zhong, F. (2015). Effect of sodium acetate and drying temperature on physicochemical and thermomechanical properties of gelatin films. *Food Hydrocolloids, 45*, 140–149. https://doi.org/10.1016/j.foodhyd.2014.10.009

Liu, F., Chiou, B. S., Avena-Bustillos, R. J., Zhang, Y., Li, Y., McHugh, T. H., et al. (2017). Study of combined effects of glycerol and transglutaminase on properties of gelatin films. *Food Hydrocolloids, 65*, 1–9. https://doi.org/10.1016/j.foodhyd.2016.10.004

Lopes, C., Antelo, L. T., Franco-Uría, A., Alonso, A. A., & Pérez-Martín, R. (2015). Valorisation of fish by-products against waste management treatments – comparison of environmental impacts. *Waste Management, 46*, 103–112. https://doi.org/10.1016/j.wasman.2015.08.017

Nooshkam, M., Varidi, M., & Bashash, M. (2019). The Maillard reaction products as food-born antioxidant and antibrowning agents in model and real food systems. *Food Chemistry, 275*, 644–660. https://doi.org/10.1016/j.foodchem.2018.09.083

Núñez-Flores, R., Giménez, B., Fernández-Martín, F., López-Caballero, M. E., Montero, M. P., & Gómez-Guillén, M. C. (2013). Physical and functional characterization of active fish gelatin films incorporated with lignin. *Food Hydrocolloids, 30*, 163–172. https://doi.org/10.1016/j.foodhyd.2012.05.017

Oun, A. A., & Rhim, J. W. (2017). Preparation of multifunctional chitin nanowhiskers/ZnO-Ag NPs and their effect on the properties of carboxymethyl cellulose-based nanocomposite film. *Carbohydrate Polymers, 169*, 467–479. https://doi.org/10.1016/j.carbpol.2017.04.042

Qiao, C., Ma, X., Zhang, J., & Yao, J. (2017). Molecular interactions in gelatin/chitosan composite films. *Food Chemistry, 235*, 45–50. https://doi.org/10.1016/j.foodchem.2017.05.045

Qin, Y., Zhang, S., Yu, J., Yang, J., Xiong, L., & Sun, Q. (2016). Effects of chitin nano-whiskers on the antibacterial and physicochemical properties of maize starch films. *Carbohydrate Polymers, 147*, 372–378. https://doi.org/10.1016/j.carbpol.2016.03.095

Rodrigues, C., Muneron de Mello, J. M., Dalcanton, F., Pier Macuvele, D. L., Padoin, N., Fiori, M. A., et al. (2020). Mechanical, thermal and antimicrobial properties of chitosan-based-nanocomposite with potential applications for food packaging. *Journal of Polymers and the Environment, 28*, 1216–1236. https://doi.org/10.1007/s10924-020-01678-y

Sahraee, S., Ghanbarzadeh, B., Milani, J. M., & Hamishehkar, H. (2017). Development of gelatin bionanocomposite films containing chitin and ZnO nanoparticles. *Food and Bioprocess Technology, 10*, 1441–1453. https://doi.org/10.1007/s11947-017-1907-2

Sahraee, S., & Milani, J. M. (2020). Chitin and chitosan-based blends, composites, and nanocomposites for packaging applications. In S. Gopi, S. Thomas, & A. Pius (Eds.), *Handbook of Chitin and Chitosan. Volume 2: Composites and Nanocomposites from Chitin and Chitosan, Manufacturing and Characterisations* (Chapter 8).

Shankar, S., Reddy, J. P., Rhim, J. W., & Kim, H. Y. (2015). Preparation, characterization, and antimicrobial activity of chitin nanofibrils reinforced carrageenan nanocomposite films. *Carbohydrate Polymers, 117*, 468–475. https://doi.org/10.1016/j.carbpol.2014.10.010

Sharma, R., Jafari, S. M., & Sharma, S. (2020). Antimicrobial bio-nanocomposites and their potential applications in food packaging. *Food Control, 112*, 107086. https://doi.org/10.1016/j.foodcont.2020.107086

Spada, A., Conte, A., & Del Nobile, M. A. (2018). The influence of shelf life on food waste: A model-based approach by empirical market evidence. *Journal of Cleaner Production, 172*, 3410–3414. https://doi.org/10.1016/j.jclepro.2017.11.071

Tsang, Y. F., Kumar, V., Samadar, P., Yang, Y., Lee, J., Ok, Y. S., et al. (2019). Production of bioplastic through food waste valorization. *Environment International, 127*, 625–644. https://doi.org/10.1016/j.envint.2019.03.076

Vilela, C., Kurek, M., Hayouka, Z., Röcker, B., Yildirim, S., Antunes, M. D. C., et al. (2018). A concise guide to active agents for active food packaging. *Trends in Food Science & Technology, 80*, 212–222. https://doi.org/10.1016/j.tifs.2018.08.006

Wang, Y., Chang, Y., Yu, L., Zhang, C., Xu, X., Xue, Y., et al. (2013). Crystalline structure and thermal property characterization of chitin from Antarctic krill (Euphausia superba). *Carbohydrate Polymers, 92*, 90–97. https://doi.org/10.1016/j.carbpol.2012.09.084

Wang, X., Guo, C., Hao, W., Ullah, N., Chen, L., Li, Z., et al. (2018). Development and characterization of agar-based edible films reinforced with nano-bacterial cellulose. *International Journal of Biological Macromolecules, 118*, 722–730. https://doi.org/10.1016/j.ijbiomac.2018.06.089

Wang, Y., Truong, T., Li, H., & Bhandari, B. (2019). Co-melting behaviour of sucrose, glucose & fructose. *Food Chemistry, 275*, 292–298. https://doi.org/10.1016/j.foodchem.2018.09.109

Wiercigroch, E., Szafraniec, E., Czamara, K., Pacia, M. Z., Majzner, K., Kochan, K., et al. (2017). Raman and infrared spectroscopy of carbohydrates: A review. *Spectrochimica Acta Part A: Molecular and Biomolecular Spectroscopy, 185*, 317–335. https://doi.org/10.1016/j.saa.2017.05.045

Yilmaz, Y., & Toledo, R. (2005). Antioxidant activity of water-soluble Maillard reaction products. *Food Chemistry, 93*, 273–278. https://doi.org/10.1016/j.foodchem.2004.09.043